Control of voltage-gated K^+ channel permeability to $NMDG^+$ by a residue at the outer pore

Zhuren Wang,[1] Nathan C. Wong,[1] Yvonne Cheng,[1] Steven J. Kehl,[2] and David Fedida[1]

[1]Departments of Anesthesiology, Pharmacology, and Therapeutics, and [2]Cellular and Physiological Sciences, University of British Columbia, Vancouver, British Columbia V6T 1Z3, Canada

Crystal structures of potassium (K^+) channels reveal that the selectivity filter, the narrow portion of the pore, is only ~3-Å wide and buttressed from behind, so that its ability to expand is highly constrained, and the permeation of molecules larger than Rb^+ (2.96 Å in diameter) is prevented. *N*-methyl-D-glucamine ($NMDG^+$), an organic monovalent cation, is thought to be a blocker of Kv channels, as it is much larger (~7.3 Å in mean diameter) than K^+ (2.66 Å in diameter). However, in the absence of K^+, significant $NMDG^+$ currents could be recorded from human embryonic kidney cells expressing Kv3.1 or Kv3.2b channels and Kv1.5 R487Y/V, but not wild-type channels. Inward currents were much larger than outward currents due to the presence of intracellular Mg^{2+} (1 mM), which blocked the outward $NMDG^+$ current, resulting in a strong inward rectification. The $NMDG^+$ current was inhibited by extracellular 4-aminopyridine (5 mM) or tetraethylammonium (10 mM), and largely eliminated in Kv3.2b by an S6 mutation that prevents the channel from opening (P468W) and by a pore helix mutation in Kv1.5 R487Y (W472F) that inactivates the channel at rest. These data indicate that $NMDG^+$ passes through the open ion-conducting pore and suggest a very flexible nature of the selectivity filter itself. 0.3 or 1 mM K^+ added to the external $NMDG^+$ solution positively shifted the reversal potential by ~16 or 31 mV, respectively, giving a permeability ratio for K^+ over $NMDG^+$ (P_{K^+}/P_{NMDG^+}) of ~240. Reversal potential shifts in mixtures of K^+ and $NMDG^+$ are in accordance with P_{K^+}/P_{NMDG^+}, indicating that the ions compete for permeation and suggesting that $NMDG^+$ passes through the open state. Comparison of the outer pore regions of Kv3 and Kv1.5 channels identified an Arg residue in Kv1.5 that is replaced by a Tyr in Kv3 channels. Substituting R with Y or V allowed Kv1.5 channels to conduct $NMDG^+$, suggesting a regulation by this outer pore residue of Kv channel flexibility and, as a result, permeability.

INTRODUCTION

Potassium (K^+) channels conduct and regulate K^+ flux across the cell membrane, and they can be exquisitely selective, generally allowing K^+ to pass across cell membranes while blocking other ion species. Crystal structures and biophysical studies have provided us with considerable insight into the mechanisms underlying K^+ channel selectivity. The crystal structures of KcsA and Kv1.2 channels have revealed a central pore that is mostly constricted over a narrow span, termed the selectivity filter, near the extracellular side of the membrane (Doyle et al., 1998; Long et al., 2005). K^+ selectivity arises mostly from two essential features of the selectivity filter structure: the carbonyl oxygen atoms lining it, which mimic the coordination of K^+ ions in water, and the protein packing around the selectivity filter that holds the pore open (Doyle et al., 1998). The diameter of the selectivity filter (~3 Å in the closed state) allows the carbonyl oxygen atoms to coordinate well with dehydrated K^+ (2.66 Å in diameter) and cuts off the permeation of larger ions (Doyle et al., 1998; Hille, 2001), which suggests sufficient structural rigidity to maintain selectivity (Jordan, 2007). Biophysical studies have attempted to deduce the size of the K^+ channel selectivity filter from the size of the largest permeant ion. The largest alkali metal ion that permeates K^+ channels is Rb^+ (2.96 Å in diameter). Cs^+ (3.38 Å in diameter) and methyl groups (4 Å in diameter) permeate very weakly or only under extreme circumstances, and this suggests a selectivity filter diameter of between 2.96 and 3.38 Å (Bezanilla and Armstrong, 1972; Hille, 1973). These data are consistent with the crystal structure, implying that the selectivity filter is not easily expanded further.

No protein is rigid, however, and not only when open must the selectivity filter conform to each ion by numerous small adjustments that may greatly improve ion–filter interaction, but global conformational changes of the channel protein can also change the dimensions of the selectivity filter (Hille, 2001; Jordan, 2007). In Kv

Correspondence to David Fedida: fedida@interchange.ubc.ca

Z. Wang's present address is Dept. of Physiology, Xi'an Jiaotong University, Xi'an, Shaanxi 710061, China.

Abbreviations used in this paper: 4-AP, 4-aminopyridine; eGFP, enhanced green fluorescent protein; HEK, human embryonic kidney; WT, wild-type.

The Rockefeller University Press $30.00
J. Gen. Physiol. Vol. 133 No. 4 361–374
www.jgp.org/cgi/doi/10.1085/jgp.200810139

channels, the most dramatic example arises when Kv channels C-type inactivate, and the channels transiently become Na^+ permeable (Starkus et al., 1997; Kiss et al., 1999; Wang et al., 2000a). This is one line of evidence that C-type inactivation makes the channel nonconducting through a localized constriction of the selectivity filter. In addition, mutated *Shaker* K^+ channels can pass through subconductance states on the way to the fully open state and during channel closing. These states, which seem to represent successive conformational steps in different subunits, also exhibit different ion selectivity (Zheng and Sigworth, 1997, 1998). Collectively, these studies strongly suggest a flexible nature of the selectivity filter, rather than a rigid cylindrical structure.

$NMDG^+$ is an organic monovalent cation that forms a linear molecule with a charged methylamine head group and a glucose-like hydrophilic tail, making it 6.4-Å wide and 12-Å long (~7.3 Å in mean diameter) (Villarroel et al., 1995). $NMDG^+$ permeation has been reported in a few ion channels, such as ATP-gated P2X channels (Khakh et al., 1999; Virginio et al., 1999; Eickhorst et al., 2002; Q. Li et al., 2005; Fujiwara and Kubo, 2006; Ma et al., 2006), epithelial Ca^{2+} channel ECaC (Nilius et al., 2000), glutamate receptor channels (Ciani et al., 1997), and some mechanosensitive channels (Shiga and Wangemann, 1995; Lawonn et al., 2003; T. Li et al., 2005; Zhang and Bourque, 2006). Recently, a slight permeation of $NMDG^+$ through voltage sensor pores has been reported in mutant Nav1.4 channels (Sokolov et al., 2007). In contrast to its permeation, block by $NMDG^+$ has been widely observed in K^+, Na^+, Ca^{2+}, and other ion channels. Internal $NMDG^+$ acts on *Shaker* channels as an open-channel blocker, impeding activation gate closure and thus prolonging deactivation (Melishchuk and Armstrong, 2001). $NMDG^+$ also produces a very rapid block of Ca^{2+}-activated K^+ channels from the inside of the membrane, but not the outside (Lippiat et al., 1998). Because it does not permeate most ion channels, $NMDG^+$ has been widely used as a substitute for permeant cations, such as K^+ or Na^+ (Heinemann et al., 1992; Perozo et al., 1992; Villarroel et al., 1995; Chen et al., 1997; Wang et al., 1999; Melishchuk and Armstrong, 2001).

Potassium channels of the Kv3 family have some unique biophysical properties among the Kv channel subfamilies. They activate at more negative potentials and have remarkably fast activation and deactivation kinetics (Rudy et al., 1999; Rudy and McBain, 2001). These gating properties mirror those of certain endogenous neuronal K^+ currents (Brew and Forsythe, 1995; Perney and Kaczmarek, 1997; Southan and Robertson, 2000; Lien and Jonas, 2003). In addition to those atypical gating properties, here we show that Kv3 channels also have unusual permeation properties, becoming permeable to $NMDG^+$ in the absence of K^+. The permeation of $NMDG^+$ implies that the selectivity filter of Kv3 channels is capable of expanding dramatically to accommodate an $NMDG^+$ ion. Furthermore, a tyrosine residue at the outer pore region (TVGYGDM**Y**) of Kv3 channels has been identified as a crucial component in the control of the permeability, suggesting that the structural support of the TVGYG sequence can be altered by changing the property of this residue.

MATERIALS AND METHODS

Molecular biology and cell culture

Two forms of rat Kv3 channels, Kv3.1 (Luneau et al., 1991b) and 3.2b (Luneau et al., 1991a), as well as human Kv1.5 (Fedida et al., 1993), were used in these experiments. The wild-type (WT) Kv3.1 and Kv1.5 R487Y/V mutant channels were separately expressed in human embryonic kidney (HEK) 293 cells to form stable lines, whereas the WT Kv3.2b, Kv3.2b P468W, WT Kv1.5, and Kv1.5 W472F/R487Y were transiently expressed in HEK 293 cells. The mammalian expression vector pcDNA3 was used for expression of the channels which were sequenced to check for errors before being used in transient transfections. HEK cells were grown in MEM with 10% fetal bovine serum at 37°C in an air/5% CO_2 incubator. For transient transfection, HEK cells were plated at 20–30% confluence on sterile glass coverslips in 25-mm Petri dishes and incubated overnight. The channel DNA was incubated with enhanced green fluorescent protein (eGFP) cDNA to identify the transfected cells efficiently (2 µg eGFP and 2 µg of channel DNA) and 3 µl LipofectAMINE 2000 (Invitrogen) in 100 µl of serum-free medium for 30 min, and then added to the dishes containing HEK 293 cells in 2 ml MEM with 10% fetal bovine serum. After 5 h of incubation, the culture medium was changed and the cells were incubated overnight before recording. Cells that expressed eGFP were selected for patch clamp experiments.

Electrophysiology

Coverslips with adherent cells were removed from the incubator before experiments and placed in a superfusion chamber (volume of 250 µl) containing the control bath solution at an ambient temperature (22–23°C). The bath solution was exchanged by switching the perfusates at the inlet of the chamber, with complete bath solution changes taking 5–10 s. Whole cell current recording and data analysis were performed using an Axopatch 200B amplifier and pClamp 8 software (MDS Analytical Technologies). Patch electrodes were fabricated using thin-walled borosilicate glass (World Precision Instruments) and fire polished to improve seal resistance. Electrodes had resistances of ~1–3 MΩ when filled with the filling solutions. Capacity compensation was routinely used in all whole cell recordings, and 80% series resistance compensation was only used when recording in excess of 5 nA of whole cell current. Measured series resistance was between 1 and 3 MΩ for all recordings. When the series resistance changed during the course of an experiment, data were discarded. A "-P/6" protocol was used for the online subtraction of the leakage and capacitive currents. The potential used for delivery of leak subtraction pulses was −90 to −110 mV. Data were filtered using a 4-pole Bessel filter with an f_c of 10 kHz and sampled at 10–100 kHz. Membrane potentials have not been corrected for small junction potentials that arose between bath and pipette solutions.

All charge measurements (Q_{on} and Q_{off}) were obtained by integrating the currents during the depolarizations (Q_{on}) and the repolarizations (Q_{off}) over sufficient time to allow the currents to return to the baseline. The time course of the decaying tail currents was fit with a single-exponential function: $a*exp(-t/\tau)+c$,

where a is the initial current amplitude, τ is the time constant, and c represents an offset. The permeability ratio P_{K^+}/P_{NMDG^+} was calculated according to the Goldman-Hodgkin-Katz equation (Hille, 2001):

$$E_{rev} = (RT/zF)\ln((P_{NMDG^+}[NMDG^+]_o+P_{K^+}[K^+]_o)/(P_{NMDG^+}[NMDG^+]_i+P_{K^+}[K^+]_i), \quad (1)$$

where E_{rev} is the reversal potential; [$NMDG^+$] and [K^+] are the concentrations of $NMDG^+$ and K^+, respectively; P_{NMDG^+} and P_{K^+} are the membrane permeability to $NMDG^+$ and K^+, respectively; z is the valence; and R, T, and F have their usual meanings. The data are presented throughout as mean ± SEM. Statistical analyses were conducting using one-way ANOVA.

For recordings of $NMDG^+$ currents, patch pipettes contained (in mM): 140 $NMDG^+$, 1 $MgCl_2$, 10 EGTA, and 10 HEPES. The solution was adjusted to pH 7.2 with HCl. The bath solution contained (in mM): 140 $NMDG^+$, 10 HEPES, 10 dextrose, 1 $MgCl_2$, and 1 $CaCl_2$ and was adjusted to pH 7.4 with HCl. Throughout, the subscripts $_i$ or $_o$ denote intra- or extracellular ion concentrations, respectively. All chemicals were from Sigma-Aldrich. All water used in these experiments was passed through organic filters and two-stage distillation before a Milli-Q de-ionizing system (Millipore) that returned water with specific resistance of ∼20 MΩ·cm at 25°C. Any contaminating K^+ or Na^+ in the water used for the solutions was below detection limits (<2.6 µM for K^+ and <2.2 µM for Na^+), measured using inductively coupled plasma optical emission spectroscopy (CANTEST). The purity of NMDG from Sigma-Aldrich was reported to be ≥99%, and there was a measured contamination of ∼33 µM K^+ and ∼14 µM Na^+ in the 140-mM $NMDG^+$ solutions (CANTEST). Because the central aim of this work was to examine the permeation of $NMDG^+$ through Kv3 channels, it was important to discount the actions of any contaminating permeant ions. For that reason, we repeated the examination of $NMDG^+$ permeation by using a highly purified $NMDG^+$ (99.9%) from Spectrum. The $NMDG^+$ from Spectrum gave rise to an undetectable level of K^+ (<2.6 µM) and 11 µM Na^+ in the140-mM $NMDG^+$ solutions. The data in Fig. S1 show that $NMDG^+$ tail currents persisted under these conditions and that the further addition of 1 mM Na^+ to the extracellular $NMDG^+$ solution reduced the observed tail current, which we explain by competition for permeation through the channel between $NMDG^+$ and this added Na^+.

Online supplemental material

The supplemental material provides further support that $NMDG^+$ ions carry the inward tail currents in the experiments with symmetrical $NMDG^+$. In Fig. S1, $NMDG^+$ tail currents persisted in the presence of highly purified $NMDG^+$ (Spectrum) solutions. Furthermore, the addition of 1 mM Na^+ to the extracellular $NMDG^+$ solution reduced the amplitude of the tail current. This phenomenon can be explained by competition for permeation through the channel between $NMDG^+$ and this added Na^+. The online supplemental material is available at http://www.jgp.org/cgi/content/full/jgp.200810139/DC1.

RESULTS

$NMDG^+$ currents recorded from HEK cells expressing Kv3 channels

Gating currents are usually much smaller than ionic currents, and to visualize them clearly, without contamination by ions passing through the pore, permeant ions are usually omitted. Data in Fig. 1 shows experiments to record Kv3 channel gating current, in which symmetrical 140 mM $NMDG^+$ was substituted for K^+ and Na^+ in the solutions, an ionic condition often used in Kv channel gating current studies (Heinemann et al., 1992; Perozo et al., 1992; Chen et al., 1997; Wang et al., 1999; Melishchuk and Armstrong, 2001). With these solutions, depolarizations failed to elicit any current in the untransfected HEK cells, confirming the abolition of cationic conductance through the endogenous K^+ channels (Fig. 1 B). When the same experiment was repeated with the HEK cells transiently expressing rat WT Kv3.2b channels, as seen in Fig. 1 C, upward transient current deflections were observed during the depolarizations. These are on-gating currents that originate from the displacement of the charged residues in voltage-sensing domains, mostly in S4 segments (Noda et al., 1984; Papazian et al., 1991; Shao and Papazian, 1993; Perozo et al., 1994). However, if the depolarization was more positive than −40 mV, when the membrane was repolarized to −100 mV, robust inward deactivating currents appeared during the repolarization. The amplitudes of the inward currents were much larger than the amplitude of the on-gating currents during the depolarizations, so that the charge returned during repolarization (Q_{off}) was much larger than that moved during the prior depolarization (Q_{on}). The magnitude of Q_{off} increased in a voltage-dependent manner when the depolarizations were over −40 mV and saturated at the potentials over ∼0 mV. The maximum Q_{off} was ∼20–30 times larger than Q_{on} (Fig. 1 E). This was an unusual finding because the gating charge moved during depolarization is expected to equal that returned during repolarization, in the absence of gating charge immobilization, as reported in many gating current studies in *Shaker* and other Kv channels (Perozo et al., 1992, 1993; Chen et al., 1997; Yang et al., 1997; Wang et al., 1999; Wang and Fedida, 2001). It was notable that the normalized G-V relationship for conducting Kv3.2b channels had a very similar voltage dependence to the Q_{off}/Q_{on} ratio (solid line through the data with $NMDG^+_{i/o}$ in Fig. 1 E).

As $NMDG^+$ was the dominant cation in the extracellular solution, the possibility that $NMDG^+$ might carry the inward currents was tested by replacement of extracellular NMDG-Cl with an equimolar concentration of TEA-Cl. Repeating the current recording on the same cell, we found with 140 mM TEA^+_o that the amplitudes of the inward tail currents were significantly reduced (Fig. 1 D), now showing similar waveforms to those off-gating currents seen in *Shaker* and Kv channels (Perozo et al., 1992, 1993; Bezanilla et al., 1994; Yang et al., 1997; Wang et al., 1999). The ratio of Q_{off} over Q_{on} was reduced to 1 or ∼0.8 when the membrane potentials were over 0 mV (Fig. 1 E), consistent with other studies (Perozo et al., 1992, 1993; Chen et al., 1997; Yang et al., 1997). Because the concentrations of Cl^- were similar in Fig. 1 (C and D), the experiment in Fig. 1 D confirmed that the inward deactivating currents in Fig. 1 C were carried by $NMDG^+$ through Kv3.2b channels.

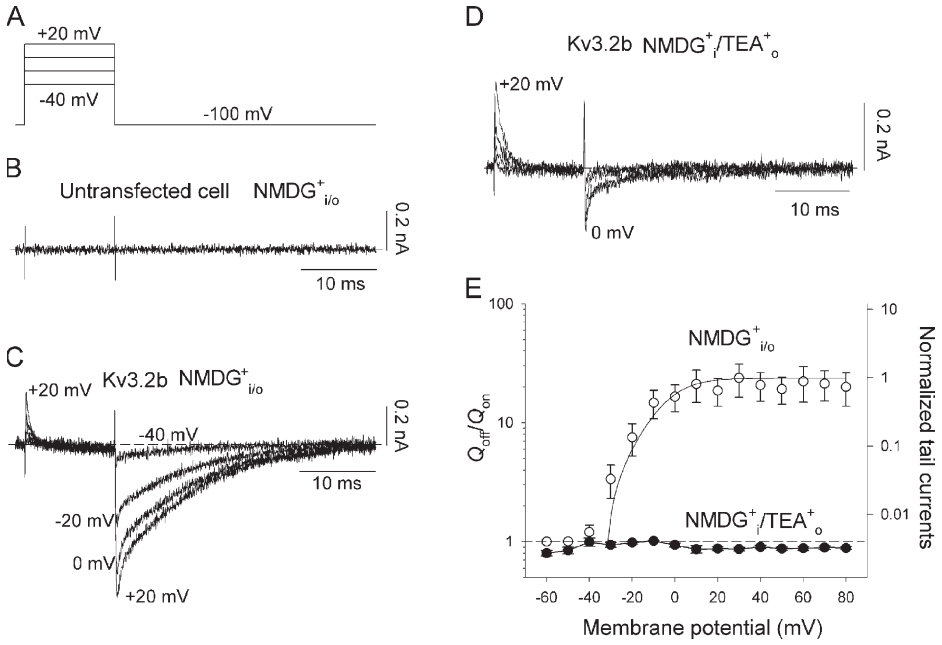

Figure 1. Inward $NMDG^+$ currents recorded from HEK cells expressing Kv3.2b channels. (A) The pulse protocol used in the experiments shown in B–D. The cells were held at −100 mV and depolarized for 12 ms to potentials between −40 and +20 mV in 20-mV steps. The depolarization was applied at 0.5 Hz. (B–D) Current recordings from an untransfected cell (B) or a cell transiently expressing Kv3.2b channels (C and D) with symmetrical 140 mM $NMDG^+$ containing solutions (B and C) or with 140 mM $NMDG^+$ containing internal solution and 140 mM TEA^+ containing external solution (D). The upward current deflections during the depolarizations in C and D are on-gating currents. The short dashed lines denote the zero current level in this and subsequent figures. (E) Averaged ratio of Q_{off}/Q_{on} as a function of the pulse potential. The amount of charge displaced during depolarization and repolarization (Q_{on} and Q_{off}) was obtained from the time integral of the currents during depolarizations and repolarizations shown in C and D ($n = 5$–8). The horizontal dotted line indicates $Q_{off}/Q_{on} = 1.0$. The solid line overlaying $NMDG^+$ data are a fitting of normalized Kv3.2b channel tail currents (right ordinate) obtained with 135 mM K^+_i/5 mM K^+_o to a single Boltzmann function. The half-activation voltage ($V_{1/2}$) was 2.3 ± 3.0 mV, and the slope factor (k) was 9.1 ± 1.0 mV ($n = 5$).

We repeated the experiments of Fig. 1 on another member of the Kv3 subfamily, rat Kv3.1 (Fig. 2). As in Fig. 1 C with symmetrical 140-mM $NMDG^+$ solutions, robust inward and slowly deactivating currents could be recorded on repolarization from the HEK cells stably expressing WT Kv3.1 channels (Fig. 2 B). The size of the inward deactivating currents became larger than the on-gating currents as the amplitudes of the depolarizing pulses exceeded −40 mV, so that the magnitude of Q_{off} was much larger than Q_{on}, with a maximum Q_{off}/Q_{on} of ∼20–30 (Fig. 2 D). When the extracellular NMDG-Cl was replaced with an equimolar concentration of TEA-Cl,

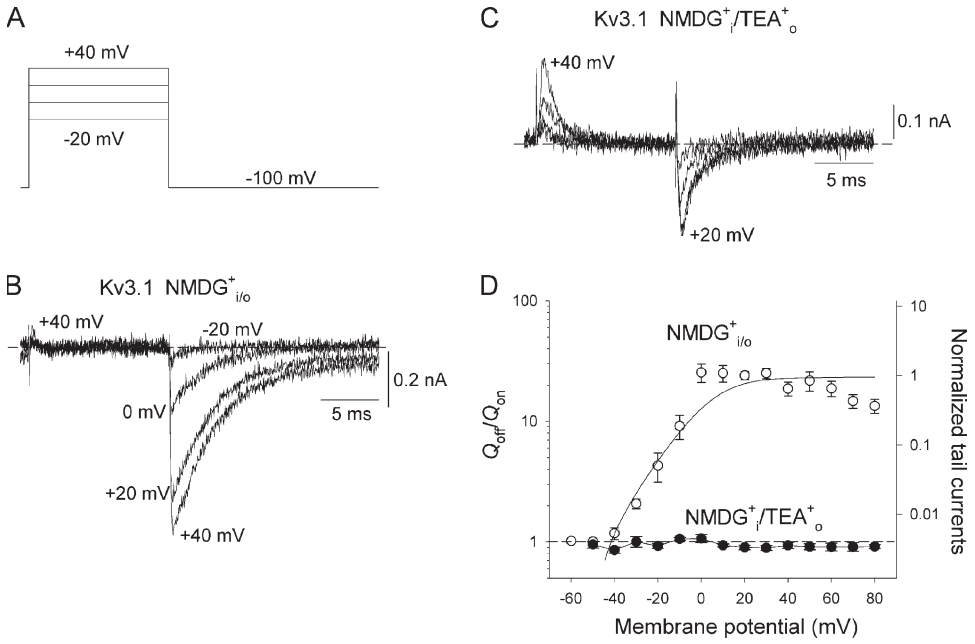

Figure 2. Inward $NMDG^+$ currents recorded from HEK cells stably expressing Kv3.1 channels. (A) The pulse protocol used to record the currents shown in B and C. The cells were held at −100 mV and depolarized for 12 ms at 0.5 Hz to potentials between −20 and +40 mV in 20-mV steps. (B and C) Current recordings from a cell stably expressing Kv3.1 channels with 140 mM of symmetrical $NMDG^+$ solutions (B) or with 140 mM $NMDG^+$ internal solution and 140 mM TEA^+ external solution (C). (D) Averaged ratio of Q_{off}/Q_{on} as a function of the pulse potentials. The amount of charge displaced during depolarizations and repolarizations (Q_{on} and Q_{off}), respectively, was obtained as described in Fig. 1 from the data shown in B and C ($n = 4$). The horizontal dotted line indicates Q_{off}/Q_{on} = 1.0. The solid line overlaying $NMDG^+$ data is a fitting of normalized Kv3.1 channel tail currents (right ordinate) obtained with 135 mM K^+_i/5 mM K^+_o to a single Boltzmann function. The half-activation voltage ($V_{1/2}$) was 3.9 ± 2.9 mV, and the slope factor (k) was 9.7 ± 0.9 mV ($n = 7$).

the amplitudes of the inward deactivating currents in Kv3.1 were reduced to the same extent as in Kv3.2b, showing normal gating currents (Fig. 2 C). The ratio of Q_{off} over Q_{on} was also reduced to ~0.9 at potentials over 0 mV (Fig. 2 D). Again, the normalized G-V relationship for conducting Kv3.1 channels had a very similar voltage dependence to the Q_{off}/Q_{on} ratio (solid line through the data with $NMDG^+_{i/o}$ in Fig. 2 D). These experiments on Kv3.2b and Kv3.1 suggest that, in the absence of K^+, extracellular $NMDG^+$ can permeate the channels upon repolarization during channel deactivation.

To further examine this permeability to $NMDG^+$, the experiment in Fig. 1 was repeated with a Kv1 family channel, Kv1.5 (Fedida et al., 1993). With symmetrical 140-mM $NMDG^+$ solutions, we failed to record any significant inward deactivating current as observed in Figs. 1 C and 2 B from HEK cells overexpressing WT Kv1.5 channels, except for the gating currents that were identical to those seen in previous studies (Wang et al., 1999; Wang and Fedida, 2001). The Q_{off}/Q_{on} ratio remained ≤1, as shown in Fig. 9 E. The experiments with Kv1.5 excluded the possibility that the inward deactivating currents shown in Figs. 1 C and 2 B resulted from ionic contamination and suggest that the permeability to $NMDG^+$ is associated with a specific Kv channel subfamily.

Block of the $NMDG^+$ currents by 4-aminopyridine (4-AP) and external TEA

A key question in this study is whether the $NMDG^+$ currents in Figs. 1 and 2 pass through the central pore of Kv3.1 and 3.2b channels or through some other pathway such as the "voltage sensor pore" (Sokolov et al., 2007). Current recordings in Fig. 3 are of Kv3.1 and Kv3.2b channels obtained with symmetrical 140-mM $NMDG^+$ solutions. Depolarizing voltage steps from the −100-mV holding potential to +80 mV (Fig. 3 A) or +40 mV (Fig. 3 B) generated significant on-gating currents and large inward deactivating $NMDG^+$ currents. 4-AP is an effective pore blocker of Kv channels, and application of 5 mM 4-AP to the bath solution had no effect on the on-gating currents, but greatly inhibited the inward $NMDG^+$ currents. The inward currents during repolarization became transient currents with a rapid decaying phase resembling off-gating currents recorded in 4-AP (McCormack et al., 1994; Fedida et al., 1996; Loboda and Armstrong, 2001). The inhibition of the inward $NMDG^+$ currents was evaluated from the Q_{off}/Q_{on} ratio, which was ~20–30 in control experiments in the absence of blockers (Figs. 1 E and 2 D). In Fig. 3, 5 mM 4-AP reduced the Q_{off}/Q_{on} ratio to 1.54 ± 0.39 ($n = 4$) in Kv3.2b and to 1.11 ± 0.08 ($n = 6$) in Kv3.1. This suggests that most, but not quite all, of the excessive inward tail current in both channels was sensitive to 4-AP.

Kv3 subfamily channels are also sensitive to block by extracellular TEA (Rudy and McBain, 2001), which binds in the outer pore and occludes the channel (MacKinnon and Yellen, 1990; Kavanaugh et al., 1991; Lenaeus et al., 2005). Fig. 4 shows current recordings of Kv3.1 and Kv3.2b channels obtained with 140 mM symmetrical $NMDG^+$ in the absence or presence of 10 mM TEA^+_o. TEA^+_o had no effect on the on-gating currents but reduced the inward $NMDG^+$ currents significantly. In Fig. 4, 10 mM TEA^+_o reduced the Q_{off}/Q_{on} ratio to 1.33 ± 0.17 ($n = 3$) in Kv3.2b and to 1.42 ± 0.34 ($n = 4$) in Kv3.1. These data, as for the 4-AP results, suggest a relatively complete block of inward $NMDG^+$ currents by TEA and support the idea that most, if not all, of the $NMDG^+$ passes through the ion-conducting pore of the channels.

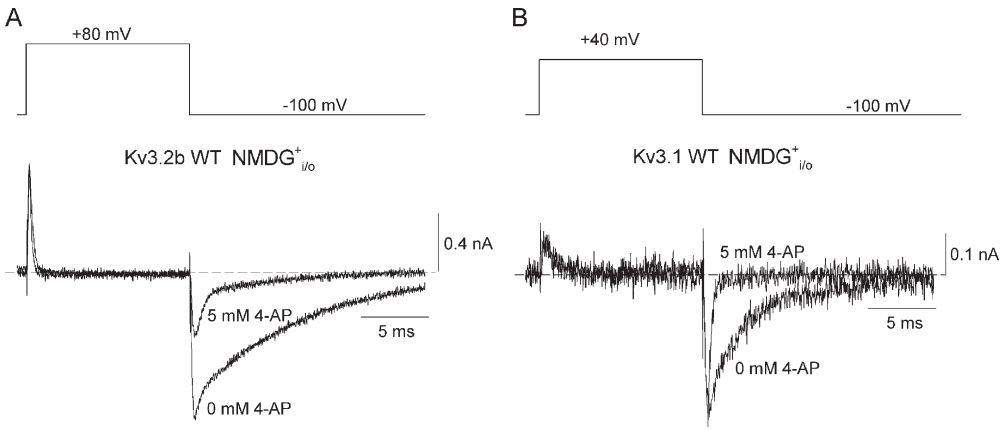

Figure 3. Inhibition of the $NMDG^+$ currents by 4-AP. Top traces of A and B illustrate the pulse protocols used to record the currents shown below. The cells were held at −100 mV and depolarized for 12 ms to +80 mV (A) or +40 mV (B). The pulse frequency was 0.5 Hz. The current recordings were obtained from a cell transiently expressing Kv3.2b channels (A) or a cell stably expressing Kv3.1 channels (B) with 140 mM of symmetrical $NMDG^+$ solutions in the presence of 0 or 5 mM 4-AP in the bathing solutions. Note that the application of 5 mM 4-AP in the bathing solutions significantly inhibited the inward $NMDG^+$ currents both in Kv3.2b and Kv3.1 channels.

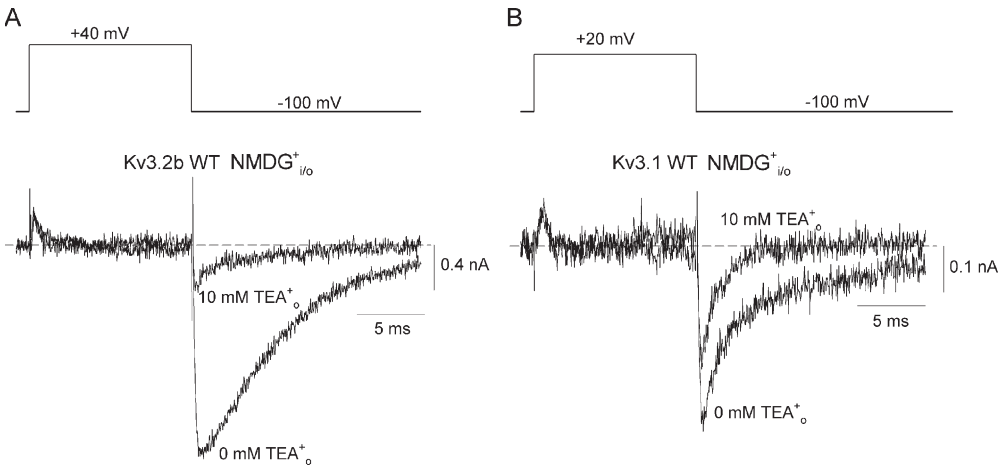

Figure 4. Block of the $NMDG^+$ currents by external TEA^+. Top traces of A and B illustrate the pulse protocols used to induce the currents shown below. The cells were held at −100 mV and depolarized for 12 ms to +40 mV (A) or +20 mV (B) every 2 s. The current recordings were obtained from a cell transiently expressing Kv3.2b channels (A) or a cell stably expressing Kv3.1 channels (B) in the presence of 0 or 10 mM TEA in the external solutions. Extracellular application of 10 mM TEA significantly blocked the inward $NMDG^+$ currents both in Kv3.2b and Kv3.1 channels.

Lack of $NMDG^+$ currents in nonconducting Kv3.2b mutant channels

Because the blocking agents used above were unable to completely inhibit $NMDG^+$ currents (as the Q_{off}/Q_{on} ratios remained significantly >1.0) and we cannot exclude their ability to bind elsewhere in the protein and block, for example, omega pores, the pathway of $NMDG^+$ permeation was further examined using nonconducting mutant channels. First, a nonconducting mutant of the rat Kv3.2b channel was created by converting P468, the first proline of the PVP motif in the S6 helix, to tryptophan (P468W; Fig. 5 A, inset). This nonconducting mutation is analogous to *Shaker* P473W (Hackos et al., 2002), in which the structural alterations of the activation gate prevent the channel from opening during activation. Transient expression of Kv3.2b P468W channels in HEK cells allows the recording of gating currents as shown in Fig. 5 A. When membrane voltage is stepped back to −100 mV, the inward currents appear as transient downward current deflections after 12-ms pulses to between −80 and +60 mV, and compared with the recordings from WT channels shown in Fig. 1 C, it is

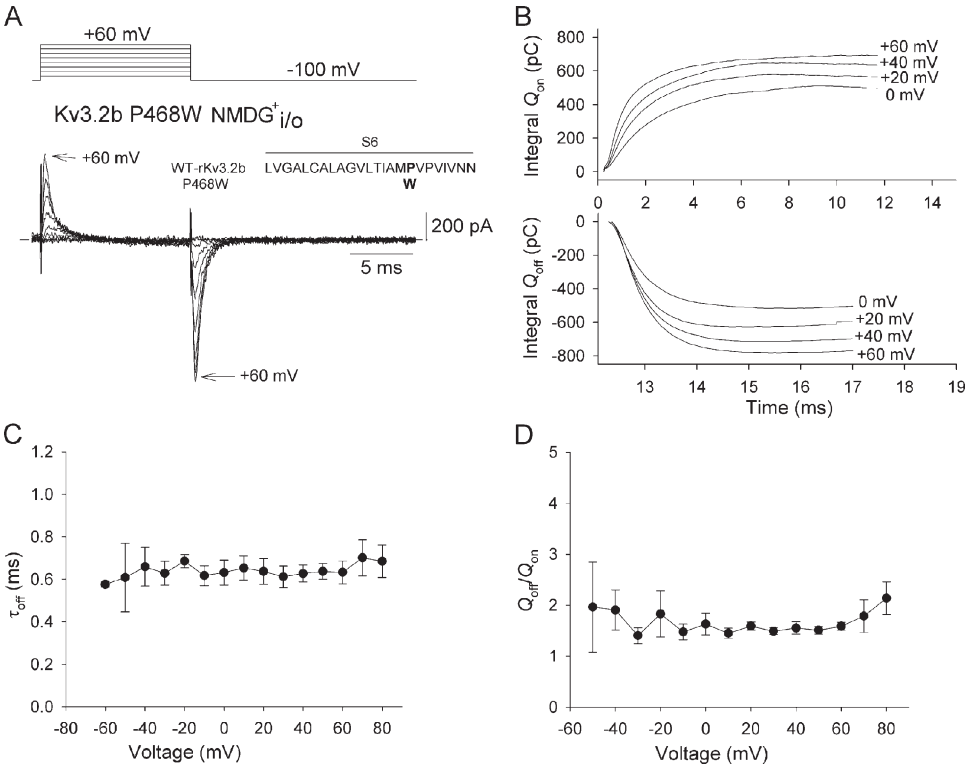

Figure 5. Lack of inward $NMDG^+$ currents in cells expressing Kv3.2b P468W channels. (A) Gating current recording from transiently expressed Kv3.2b P468W channels using the pulse protocol shown at the top of A. The interpulse interval was 5 s. (Insets) Sequence of S6 helix of the Kv3.2b subunit with the mutated proline in bold. (B) The time courses of the charge movement during the pulses (top) and upon repolarization (bottom) for Kv3.2b P468W channels. The amount of charge (Q_{on} and Q_{off}) was calculated by integrating the currents during depolarizations and repolarizations shown in A. (C) Time constants for decay of the inward tail currents as a function of pulse potential from data as in A. (D) The ratio of Q_{off}/Q_{on} as a function of pulse potential from data as in A.

obvious that the large inward currents during repolarization seen there have been eliminated in this S6 mutant channel. The amplitude of the inward tail current was only modestly larger than the amplitude of on-gating current with an averaged ratio of Q_{off}/Q_{on} of 1.5–2 over the range of voltages from −50 to +80 mV (Fig. 5, B and D), much less than that in Fig. 1 E. In addition, the inward tail currents remained fast with monoexponential kinetics during the decay. The time constant of relaxation of the inward tail current (τ_{off}) was ~0.6 ms over the range of voltages from −60 to +80 mV (Fig. 5 C). Such transient inward currents during repolarization resemble off-gating currents recorded in 4-AP (McCormack et al., 1994; Fedida et al., 1996; Loboda and Armstrong, 2001), consistent with the suggestion that the P468W mutation prevented the opening of the activation gate during the prior depolarization. Hence, the lack of significant inward $NMDG^+$ current in the Kv3.2b P468W mutant channel resulted from the closing of the activation gate, supporting the idea that the permeation path for $NMDG^+$ ions is the central ion-conducting pore, i.e., through the selectivity filter.

The second mutation of Kv3.2b that we attempted to use to identify the pathway for $NMDG^+$ permeation was in the pore, W426F, which is analogous to the *Shaker* W434F (Perozo et al., 1993) and Kv1.5 W472F (Wang et al., 1999) nonconducting mutants. The mutation of W to F makes the channels inactivated at rest, blocking the permeation of cations larger than Na^+ through the selectivity filter (Yang et al., 1997; Starkus et al., 1998; Wang and Fedida, 2001). However, transient expression of Kv3.2b W426F with eGFP in HEK cells gave neither gating current nor $NMDG^+$ current from the cells showing significant expression of eGFP protein. This might suggest that the inactivated mutant channel no longer conducted $NMDG^+$, but we could not exclude the possibility that Kv3.2b W426F did not express at the cell surface. As we could not conclusively establish whether or not the $NMDG^+$ current was abolished in Kv3.2b W426F channels, Kv1.5 was used as an alternative model to examine the effect of this pore mutation on $NMDG^+$ permeation (see Fig. 9).

Block of the outward $NMDG^+$ current by intracellular Mg^{2+}

Kv3.1 and 3.2b channels conducted large inward $NMDG^+$ currents during channel deactivation (Figs. 1–4), but strong depolarizations failed to evoke such large outward $NMDG^+$ currents, despite equal intracellular and extracellular $NMDG^+$ concentrations. Cells expressing Kv3.1 channels, in symmetrical 140 mM $NMDG^+$, were held at −100 mV and depolarized by a prepulse to +60 mV for 30 ms to activate the channels, and then the cell was repolarized to −60 mV for 2 ms, followed by a second depolarizing pulse to +60 mV. During the prepulse, on-gating current at the beginning of the pulse was followed by a slowly rising outward current that reached ~200 pA. Upon repolarization to −60 mV, the peak amplitude of the inward current was over 1 nA, giving a ratio of the outward current to the inward current of 0.11 (mean ratio: 0.07 ± 0.02;

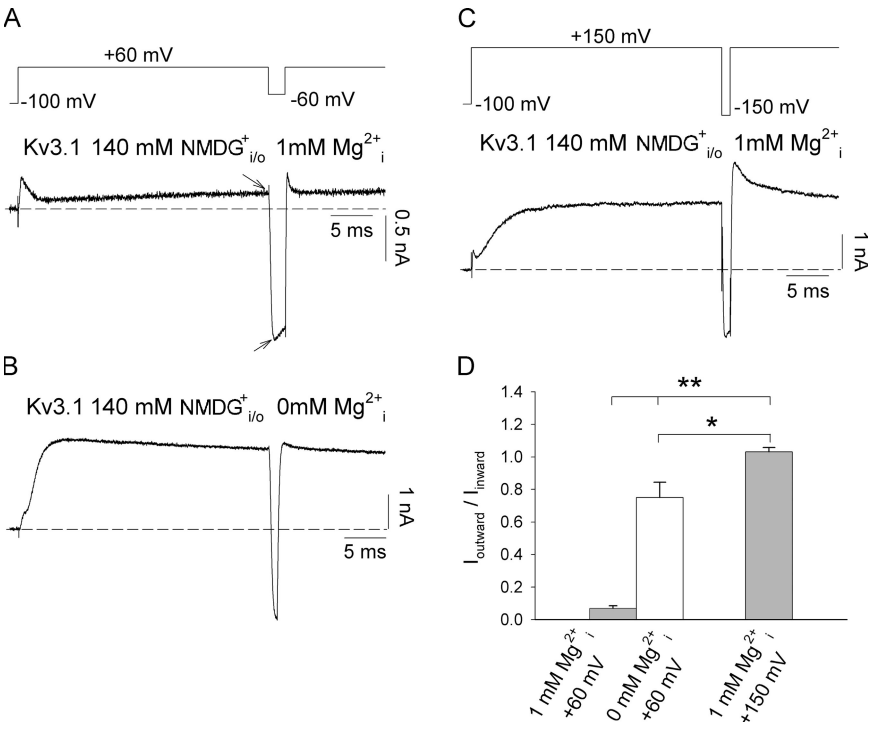

Figure 6. Block of the outward $NMDG^+$ current by internal Mg^{2+}. (A) A current recording from a cell stably expressing Kv3.1 channels with symmetrical 140 mM $NMDG^+$, 1 mM Mg^{2+} solutions. The double-pulse protocol used to elicit the currents in A and B is shown at the top of A. The cells were held at −100 mV. A depolarizing pulse to +60 mV was interrupted by a short repolarizing pulse to −60 mV to assess the inward currents. (B) A current recording obtained with similar experimental conditions as in A except for the absence of internal Mg^{2+}. (C) A current recording obtained with similar experimental conditions as in A. The double-pulse protocol used to elicit these currents is shown at the top of C. The cells were held at −100 mV, and then depolarized to +150 mV, interrupted by a short repolarizing pulse to −150 mV to assess the inward currents. (D) The averaged ratio of the outward current over the inward current in the absence or presence of internal Mg^{2+}. The amplitude of the outward and inward currents was measured at the end of the prepulse and the beginning of the repolarizing pulse as indicated by arrows in A. The data are from four to five cells. *, $P < 0.01$; **, $P < 0.001$.

n = 4; Fig. 6 D). Returning to +60 mV again showed only a small outward current, so these data suggest that the $NMDG^+$ current in Kv3 channels shows strong inward rectification.

In inward rectifier K^+ channels, the rectification results from the rapid block of the pore by intracellular Mg^{2+} and/or polyamine molecules (Horie et al., 1987; Matsuda et al., 1987; Nichols and Lopatin, 1997). Such block of the pore by internal Mg^{2+} at positive potentials was also observed in Kv3.1 K^+ current recordings (Harris and Isacoff, 1996; Friederich et al., 2003). The experiment shown in Fig. 6 A was repeated using a Mg^{2+}-free internal solution (Fig. 6 B), and here the +60-mV pulse induced a significantly larger outward $NMDG^+$ current that had a mean amplitude ratio of 0.75 ± 0.09 (n = 4) to the inward current (Fig. 6 D). As Mg^{2+} ions are smaller (diameter: 1.3 Å) (Hille, 2001) than $NMDG^+$, we wondered if Mg^{2+} could also pass through Kv3 channels. Fig. 6 C shows that in 1 mM of Mg^{2+}-containing internal solution, a depolarizing pulse to +150 mV equalized the mean amplitude ratio of inward to outward currents (1.03 ± 0.03; n = 5; Fig. 6 D), indicating that the internal Mg^{2+} block was relieved by large depolarizations that forced Mg^{2+} ions through the pore.

Kv3 channels conduct $NMDG^+$ in their open state

The experiments described so far clearly suggest that $NMDG^+$ permeates through the pore of Kv3 channels, rather than via another secondary pathway. However, they do not establish the nature of the conducting channel state. Potassium channels are typically highly selective for K^+ ions over other cations in their open state, but the ion selectivity of K^+ channels is altered along with conformational changes of the channel protein. One example is C-type inactivated *Shaker* and Kv channels that do not pass significant amounts of K^+, but become permeable to Na^+ (Starkus et al., 1997; Kiss et al., 1999; Wang et al., 2000a). As well, in the absence of internal and external K^+, *Shaker* and some Kv channels show rapid increases in Na^+ permeability as a result of accelerated C-type inactivation. Because many of the experiments we describe here were performed in the absence of internal or external K^+, it is possible that although slow inactivation appears absent in these channels, it may be enhanced in the absence of K^+ (Wang and Fedida, 2001), and thus that $NMDG^+$ currents are passing through inactivated channels. Interestingly, it is thought that 4-AP cannot block inactivated channels (Castle et al., 1994), so the observation that 4-AP blocks $NMDG^+$ currents quite effectively (Fig. 3) argues against

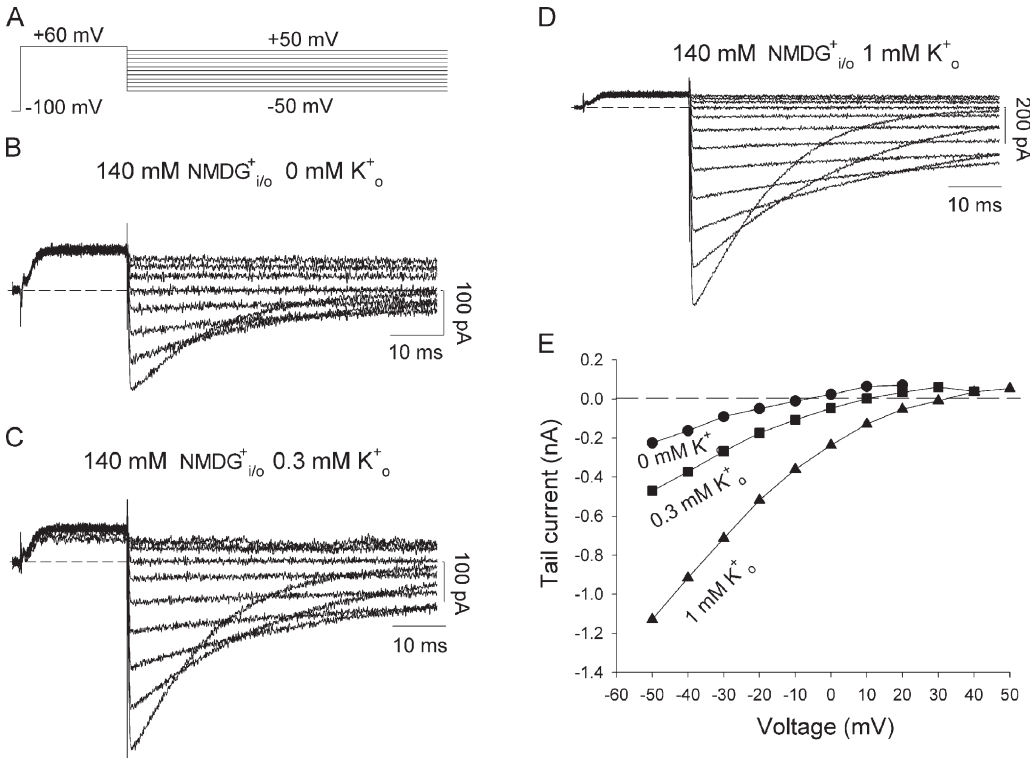

Figure 7. Changes in the reversal potential of $NMDG^+$ currents with the addition of low concentrations of K^+_o. (A) The pulses used for the experiments shown in B–D. A depolarizing step from −100 to +60 mV was followed by repolarization to different potentials ranging from −50 to +20, +40, and +50 mV in B–D, respectively. The pulses were applied at 0.1 Hz. (B–D) Currents recorded in the presence of symmetrical 140 mM $NMDG^+_{i/o}$ plus the concentration of K^+_o indicated in the figure. The internal solutions were Mg^{2+} free in all experiments. (E) Peak tail current–voltage curves showing the shift in reversal potential produced by the addition of 0.3 or 1 mM of extracellular K^+. Data from B–D: n = 4.

the channels being C-type inactivated and supports the hypothesis that they are in the open state.

If the permeation of $NMDG^+$ is through the open Kv3 channel pore, $NMDG^+$ and K^+ ions will occupy the conduction pathway, so mixtures of $NMDG^+$ and K^+ should produce one of two possible changes of the reversal potential. If permeation of $NMDG^+$ and K^+ through the channel is mutually exclusive, the reversal potential for the currents should be at the equilibrium potential of one of the ions. On the other hand, if both K^+ and $NMDG^+$ can permeate open Kv3 channels at low concentrations of K^+, mixtures of K^+ and $NMDG^+$ should show an intermediate reversal potential, governed by the permeability ratio, P_{K^+}/P_{NMDG^+}, of the two ions. With 140 mM $NMDG^+$ inside and outside the membrane, the extracellular addition of 0.3 or 1 mM K^+ positively shifted the reversal potential, measured from the tail currents shown in Fig. 7 (B–D), from -5.5 ± 1.6 mV to 10.2 ± 0.8 and 25.2 ± 1.8 mV, respectively ($n = 4$; $P < 0.001$; Fig. 7 E). At the same time, the P_{K^+}/P_{NMDG^+} ratio, calculated from GHK constant field theory as described in Materials and methods, remained almost the same in the presence of 0.3 and 1 mM K^+_o, at 232 ± 23.0 and 242 ± 24.8, respectively. The current waveforms during these experiments, particularly with 1 mM K^+_o, strongly suggests that $NMDG^+$ permeates open Kv3 channels, as it is extremely unlikely that channels could shift from an inactivated state passing outward $NMDG^+$ current to the open state to allow observation of inward K^+ tail currents without complex kinetic changes.

Reversal potential shifts in Kv3.1 were further measured using mixtures of K^+ and $NMDG^+$ (Fig. 8). Solutions contained 1 mM K^+_i/0.3 mM K^+_o plus 140 mM $NMDG^+_{i/o}$, 10 mM K^+_i/3 mM K^+_o plus 140 mM $NMDG^+_{i/o}$, and 100 mM K^+_i plus 40 mM $NMDG^+_i$/30 mM K^+_o plus 110 mM $NMDG^+_o$. As the ratio of K^+_o/K^+_i was maintained at 0.3, the reversal potential for K^+ (E_{K^+}), calculated with the Nernst equation, should remain at ~ -30 mV in the absence of $NMDG^+$ permeation. With 1 mM K^+_i/0.3 mM K^+_o plus 140 mM $NMDG^+_{i/o}$, the reversal potential, measured from the tail currents, was -14.4 ± 0.8 mV ($n = 7$). The reversal potential was not equal to E_{K^+} but was consistent with the value (~ -14 mV) calculated from the GHK equation using P_{K^+}/P_{NMDG^+} equal to 232. Increases in K^+ concentration produced a shift of the reversal potential toward E_{K^+}, so that with 100 mM K^+_i /30 mM K^+_o, the reversal potential became -28.0 ± 2.0 mV ($n = 11$), almost equal to E_{K^+} and the value (~ -30 mV) calculated from the GHK equation. The reversal potential shifts in the different mixtures of K^+ and $NMDG^+$ strongly suggest that $NMDG^+$ permeates open Kv3 channels.

We also measured the permeability of Kv3.1 channels to another larger cation, Cs^+, which has a diameter of 3.38 Å and usually is considered a blocker of most K^+ channels, to confirm the capability of Kv3 channels to conduct large cations. Significant Cs^+ current could be recorded from HEK cells expressing WT Kv3.1 channels. The P_{K^+}/PCs^+ ratio in the presence of 70, 100, and 140 mM K^+_o (Cs^+_i = 140 mM) was 3.3 ± 0.3, 3.8 ± 0.2, and 3.9 ± 0.2 ($n = 6$–9), respectively.

$NMDG^+$ permeability controlled by an Arg at the outer pore

To date, significant $NMDG^+$ conductance has not been reported in any Kv channels. Here, apart from demonstrating

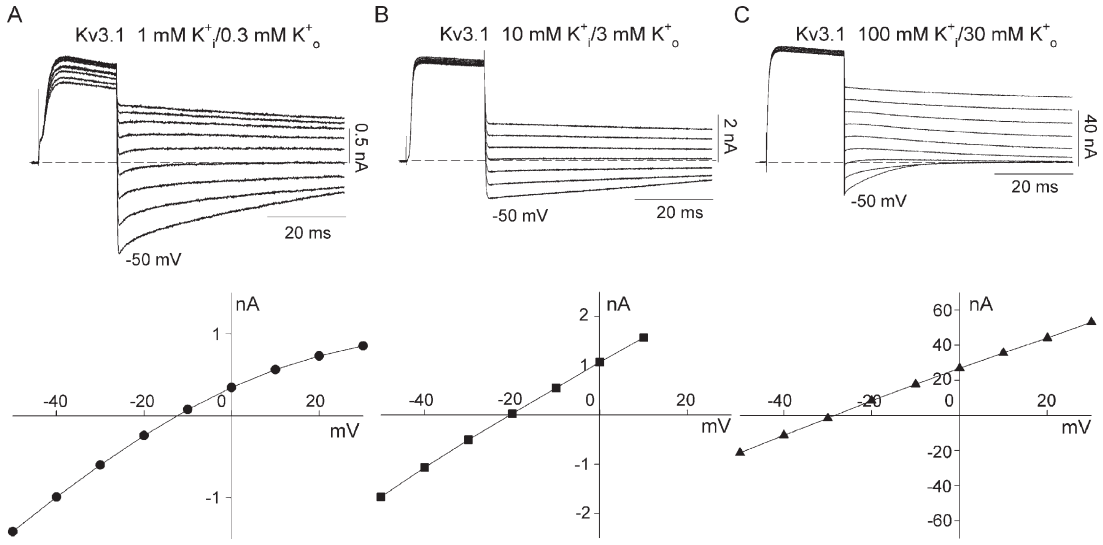

Figure 8. Shifts of the Kv3.1 reversal potential in different mixtures of $K^+_{i/o}$ and $NMDG^+_{i/o}$. (A–C; Top) Currents recorded in the presence of symmetrical 140 mM $NMDG^+_{i/o}$ (A and B) or 40 mM $NMDG^+_i$ and 110 mM $NMDG^+_o$ (C) plus the concentration ratios for K^+ indicated above the traces in A–C. The pulse protocol used for the experiments is similar to that shown in Fig. 7 A. The internal solutions were Mg^{2+} free in all experiments. (A–C; bottom) Peak tail current–voltage curves showing the shift in reversal potential in mixtures of K^+ and $NMDG^+$. The reversal potentials were -12.3 (-14.4 ± 0.8 mV; $n = 7$), -20.6 (-20.6 ± 1.2 mV; $n = 6$), and -28.8 mV (-28.0 ± 2.0 mV; $n = 11$) for A, B, and C, respectively. The differences between A, B, and C are all highly significant ($P < 0.001$).

a significant $NMDG^+$ permeability in Kv3 channels, we also confirmed the lack of $NMDG^+$ conductance in a Kv1 family channel, Kv1.5. This led us to compare the amino acid sequences in the pore of Kv3 and Kv1.5 channels to attempt to identify a molecular mechanism underlying the permeability to $NMDG^+$. The pore helix and selectivity filter region are highly conserved, and only four differences are seen between Kv3.1, Kv3.2b, and Kv1.5 (Fig. 9 A). One of these is an Arg residue located at the outer pore region in Kv1.5 (R487), which is the positional equivalent of T449 in *Shaker*. In Kv3.1 and Kv3.2b, this is replaced by a Tyr residue that confers a high affinity to extracellular TEA^+ binding (MacKinnon and Yellen, 1990; Fedida et al., 1999) and is suggested to inhibit C-type inactivation in Kv channels (Lopez-Barneo et al., 1993; Liu et al., 1996). Particularly, substitution of Val for Arg (R487V) prevents the inactivation of Kv1.5 Na^+ current (Wang et al., 2000b). These data suggest that this residue can critically regulate the conformation of the outer pore mouth and the selectivity filter and, perhaps in doing so, regulate channel permeability.

Mutation of the Arg residue in Kv1.5 (R487) to either Tyr (Kv1.5 R487Y) or Val (Kv1.5 R487V) conferred $NMDG^+$ permeability to mutant Kv1.5 channels expressed in HEK cells. Both single mutants showed large inward $NMDG^+$ currents during repolarization to −100 mV (Fig. 9, B and C), which were similar to those seen in Kv3.1 and Kv3.2b channels. The amplitudes of the inward currents were much larger than the amplitude of the on-gating currents during the preceding depolarizations. The averaged ratio of Q_{off} over Q_{on} increased in a voltage-dependent manner to as much as 30 when the depolarizations were positive to −40 mV and saturated at potentials over −10 mV (Fig. 9 E). These inward currents could also be abolished by replacement of $NMDG^+_o$ with TEA^+_o (not depicted).

The result with the mutants Kv1.5 R487V/Y, which are thought to cause relatively local changes in selectivity filter function, provides further support to our data showing that the selectivity filter pathway provides the route for $NMDG^+$ current. We tested this idea using the pore mutant, Kv1.5 W472F, which is equivalent to *Shaker* W434F (Perozo et al., 1993), and permanently inactivates the channel at rest. As in *Shaker*, Kv1.5 W472F mutant channels do not allow cations larger than Na^+ to pass through their selectivity filter (Wang and Fedida, 2001, 2002). With symmetrical 140 mM $NMDG^+_{i/o}$, recordings from cells expressing Kv1.5 W472F/R487Y only showed gating currents that were identical to those previously characterized from WT, W434F, or W472F mutants of *Shaker* and Kv1.5 channels, respectively (Perozo et al., 1992, 1993; Yang et al., 1997; Wang et al., 1999;

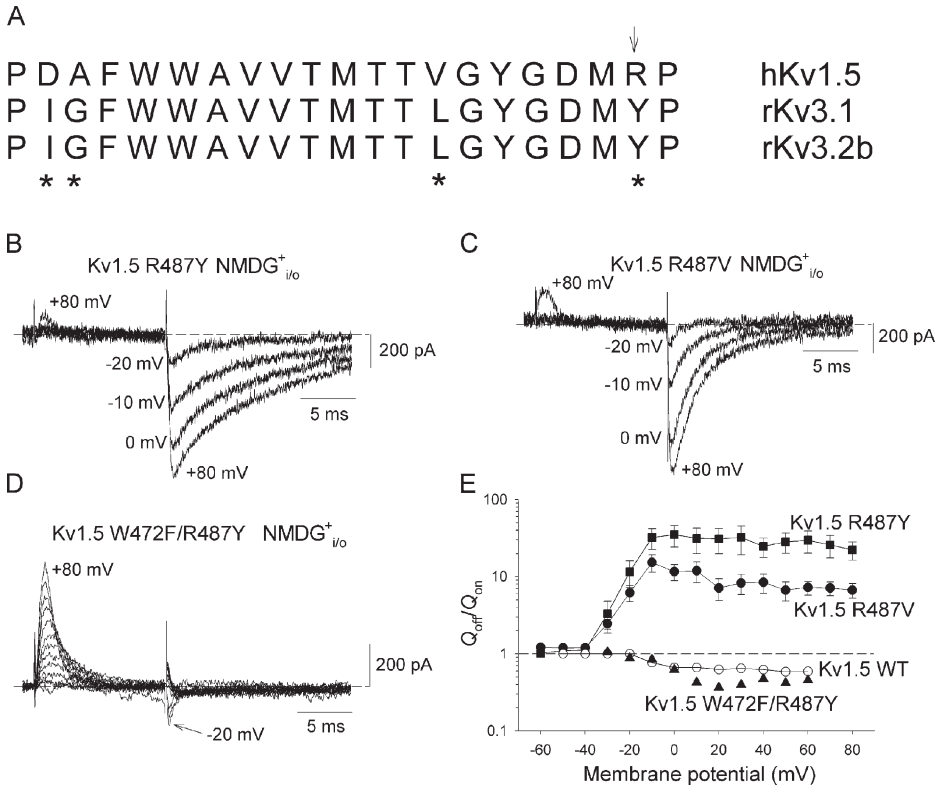

Figure 9. $NMDG^+$ currents recorded from HEK cells expressing Kv1.5 R487Y/V or Kv1.5 W472F/R487Y mutant channels. (A) Sequence alignment of the P-loop region of Kv1.5, Kv3.1, and Kv3.2b channels. The asterisks mark the amino acid differences between the three sequences. An arrow indicates an Arg residue at the outer pore of Kv1.5, which is replaced by Tyr in Kv3.1 and Kv3.2b channels and is the positional homologue of *Shaker* T449. (B and C) Current recordings from HEK cells stably expressing Kv1.5 R487Y (B) or R487V (C) mutant channels. To record the currents, the cells were held at −100 mV and depolarized for 12 ms at 0.5 Hz to potentials of −20, −10, 0, and +80 mV. The experimental solutions are similar to those in Fig. 1 C. The upward current deflections during the depolarizations are on-gating currents. (D) Gating current recording from transiently expressed Kv1.5 W472F/R487Y channels with pulses from −60 to +80 mV in 10-mV steps. The holding potential was −100 mV, and pulses were applied at 0.5 Hz. (E) Averaged ratio of Q_{off}/Q_{on} as a function of the pulse potential. The amount of charge displaced during depolarization and repolarization (Q_{on} and Q_{off}, respectively) was obtained from the time integral of the currents during depolarization and repolarization shown in B, C, and D as indicated by the label on each graph ($n = 5$). Kv1.5 WT data are included for comparative purposes.

Wang and Fedida, 2001) (Fig. 9 D). Off-gating currents were decreased in amplitude at potentials >−20 mV (Fig. 9 E), and this relative gating charge immobilization further emphasized the abolition of the large inward $NMDG^+$ currents seen in Kv1.5 R487Y/V channels (Fig. 9, B and C). Clearly, the pore mutation W472F blocked the permeation of $NMDG^+$, despite the presence of a Tyr at 487, and further, the lack of $NMDG^+$ current through the permanently inactivated W472F channels strongly suggested that $NMDG^+$ conduction in the Kv3 and Kv1.5 R487Y/V channels cannot be through inactivated channels, but must be through the ion-conducting pore in its open state.

DISCUSSION

Permeation of $NMDG^+$ in Kv3 channels

Here, we describe a novel permeability to $NMDG^+$ in Kv3.1, 3.2b, and Kv1.5 R487Y/V channels. $NMDG^+$ is a much larger molecule than K^+, and the ability of the pore to allow $NMDG^+$ to permeate suggests a significant flexibility in the structure of the selectivity filter, more so than previously thought, and we ascribe this regulation of selectivity filter diameter to a residue external to the filter itself. In this study, the permeability to $NMDG^+$ was tested in rat Kv3.1 and Kv3.2b channels, but because the composition of amino acids is very conserved in the pore region of Kv3 channels (Rudy et al., 1999; Shealy et al., 2003), it is very likely that all Kv3 subfamily channels share this permeability to $NMDG^+$.

Asymmetrical gating currents in Kv3 channels inhibited by 4-AP and TEA

This work began with unusual gating current recordings from HEK cells expressing WT Kv3.1 and 3.2b channels. With the symmetrical $NMDG^+$ solutions that are often used, the recorded "off-gating currents" were much larger than the on-gating currents at the voltages over the activation threshold (Figs. 1 C and 2 B), showing a larger amount of charge returned during deactivation than moved during activation (Figs. 1 E and 2 D). Such gating current recordings are different from those obtained from *Shaker* and other Kv channels, in which the Q_{off} is usually equal to or less than Q_{on} (Perozo et al., 1992, 1993; Bezanilla et al., 1994; Chen et al., 1997; Yang et al., 1997; Wang et al., 1999). It is clear that the larger tail currents obtained in Kv3 channels were not due to any contamination from the endogenous channels, and that they could be reduced to a magnitude equal to or less than the on-gating currents by replacing $NMDG^+_o$ with TEA^+_o (Figs. 1 and 2). These data suggested that the larger tail currents resulted from contamination by ionic $NMDG^+$ currents during repolarization. Both 4-AP and TEA^+_o could inhibit the inward $NMDG^+$ currents (Figs. 3 and 4), and mutations made in the deep pore or at the activation gate to prevent the ions from entering the selectivity filter also successfully abolished the $NMDG^+$ current (Figs. 5 and 9), suggesting that $NMDG^+$ passed through the ion-conducting pore of the channels. Because $NMDG^+$ currents had a voltage dependence that matched channel opening rather than Q_{on}, this also suggests that they are associated with pore opening rather than a secondary conduction pathway.

Intracellular Mg^{2+}_i block of $NMDG^+$ currents

Internal Mg^{2+} strongly blocks the outward $NMDG^+$ current (Fig. 6). Mg^{2+}_i has also been reported to produce a small block of macroscopic K^+ current at very positive potentials (Friederich et al., 2003), but this seems less significant than the block of $NMDG^+$ current seen here. This may not be directly related to the different ionic diameters because although Mg^{2+} is roughly half the diameter of K^+, fully hydrated Mg^{2+} is somewhat bigger (∼10 Å) (Lunin et al., 2006) than a hydrated K^+, which is ∼8 Å in diameter (Yang and Sachs, 1990; Khodakhah et al., 1997). It is possible that hydrated Mg^{2+} in the inner vestibule provides a more effective barrier preventing $NMDG^+$ access to the selectivity filter than it does for K^+. Interestingly, we found that the block of outward $NMDG^+$ current by internal Mg^{2+} ions could be relieved by very large depolarizations, which suggested that Mg^{2+} needed to overcome a large energy barrier to pass through the selectivity filter, perhaps one required to dehydrate Mg^{2+} ions. Of course, we cannot rule out the possibility that strong depolarizations can deform the selectivity filter structure and allow permeation.

$NMDG^+$ conduction through the open channel

The selectivity of Kv channels varies with conformation, giving state-dependent ion selectivity. C-type inactivated *Shaker* and Kv channels are impermeable to K^+ but become more conductive to Na^+, implying a conformational change involving a partial constriction of the selectivity filter (Starkus et al., 1997; Kiss et al., 1999; Wang et al., 2000a). Because $NMDG^+$ currents were recorded in the absence of K^+ (Figs. 1 and 2), conformational and functional changes such as enhanced C-type inactivation might have occurred (Starkus et al., 1997; Wang et al., 2000a; Wang and Fedida, 2001). The addition of 0.3 and 1 mM K^+ to the external $NMDG^+$ solution positively shifted the reversal potential from −5.5 mV for symmetrical $NMDG^+$ to +10.2 and +25.2 mV (Fig. 7), with little change in P_{K^+}/P_{NMDG^+}. This permeability ratio (P_{K^+}/P_{NMDG^+}) also governed the shifts of reversal potential in the mixtures of K^+ and $NMDG^+$ (Fig. 8). These observations can be explained by a permeation of both $NMDG^+$ and K^+ ions through Kv3 channels in their open state. Alternatively, if channels were inactivated or in other states that allowed $NMDG^+$ but not K^+ permeation, low concentrations of K^+ might produce a block of $NMDG^+$

permeation without itself conducting, but would not change the observed reversal potential.

$NMDG^+$ conduction through the open state was further supported by experiments with the Kv1.5 W472F/R487Y channel (Fig. 9, D and E). As the Kv1.5 W472F mutation permanently inactivates channels, the failure to record $NMDG^+$ current from cells expressing the construct strongly indicates that the inactivated channels were unable to conduct $NMDG^+$.

Expansion of the narrow selectivity filter

The crystal structures of KcsA and Kv1.2 channels show that the open intracellular gate can be as wide as 10 Å, and the deeper internal cavity has a diameter of ~10 Å (Doyle et al., 1998; Long et al., 2005), so that neither of these structures should be a barrier for the entry of $NMDG^+$ to the base of the selectivity filter. The selectivity filter itself is lined by backbone carbonyl oxygen atoms, approximating the hydration shell of K^+ ions, and the Val and Tyr side chains from the V-G-Y-G sequence point away from the pore and make specific interactions with side chains of amino acids from the tilted pore helix. These structural constraints hold the selectivity filter open at its proper diameter (Doyle et al., 1998), as wide as only one or two atomic diameters. Such a narrow pore allows the carbonyl oxygen atoms to coordinate dehydrated K^+ ions, but not smaller Na^+ ions, to give the selectivity over Na^+ seen in K^+ channels. The number of carbonyl oxygen atoms that surround permeating ions is the most important factor in determining ion selectivity (Varma and Rempe, 2007), so there must be sufficient structural rigidity to maintain the carbonyl ligation environment. Consequently, a selectivity filter one or two atomic diameters wide cuts off the permeation of larger particles. Biophysical studies show that the largest permeant metal ion in K^+ channels is Rb^+, suggesting a selectivity filter with a maximum inner diameter of around 3 Å (Bezanilla and Armstrong, 1972; Hille, 1973), which is in good agreement with data from the crystal structures of KcsA and Kv1.2 channels (Doyle et al., 1998; Long et al., 2005). The sharpness of the permeability cutoff for K^+ channels implies that the selectivity filter is not easily expanded further.

The permeability to $NMDG^+$ observed in Kv3 channels is therefore surprising, suggesting an expansibility or plasticity of the selectivity filter in Kv channels. Such a dramatic enlargement of the pore, similar to the phenomenon reported in some P2X channels (Khakh et al., 1999; Virginio et al., 1999), has never been reported in Kv channels. There is only one amino acid difference between the filter sequence of Kv1.5 and Kv3 channels, TVGYG in Kv1.5 and TLGYG in Kv3 channels (Fig. 8 A), and it seems unlikely that a single change of V to L would make the selectivity filter of Kv3 channels better able to conduct $NMDG^+$ than Kv1.5 because of their chemical similarity. Alternatively, the protein packing around the selectivity filter could be an important factor in allowing flexibility of the selectivity filter, as suggested by crystal structure and biophysical studies (Doyle et al., 1998; Cordero-Morales et al., 2007). And indeed, the data in the present study suggest an important role for Tyr residues in the outer pore.

Control of the permeability by an outer pore residue

A Tyr residue in the outer pore of Kv3 channels (Y407 in Kv3.1 and Y444 in Kv3.2b) appears to be responsible for the permeability to $NMDG^+$, as Kv1.5 with an Arg at the equivalent site, R487, does not conduct $NMDG^+$ at all (Wang et al., 1999), whereas mutation of Arg to either Tyr or Val in Kv1.5 R487Y/V allows $NMDG^+$ permeation (Fig. 9). The equivalent residue in *Shaker* (T449) was originally identified as part of the high affinity TEA binding site (MacKinnon and Yellen, 1990). Mutation of T to Y results in even higher affinity TEA^+ binding, whereas mutation of T to a charged residue results in a loss of external TEA^+ sensitivity as exemplified in Kv1.5. The mechanisms underlying external TEA^+ binding are well understood from biophysical, pharmacological, and crystal structure studies (MacKinnon and Yellen, 1990; Kavanaugh et al., 1991; Lenaeus et al., 2005). The aromatic side chains of Y or the aliphatic hydroxyl side chain of T form a receptor for TEA^+ where it can bind and occlude the pore. All Kv3 subfamily channels have a Tyr residue at the equivalent site (Rudy et al., 1999; Shealy et al., 2003) and are very sensitive to external TEA^+ (Rudy et al., 1999; Rudy and McBain, 2001).

The interaction between outer pore and pore helix residues has also been suggested to be key in initiating and stabilizing the constriction of the selectivity filter during C-type inactivation (Cordero-Morales et al., 2007). We also noted that when Kv3.1 channels conduct Na^+ current, C-type inactivation is reduced (not depicted) as in Kv1.5 R487V/Y mutant channels (Wang et al., 2000b). And so, it seems that this Tyr residue plays a similar role in determining many of the biophysical and pharmacological properties of Kv3 channels as it does in *Shaker* and other Kv1 channels. The molecular mechanisms underlying the $NMDG^+$ permeability of Kv3 channels remain to be fully understood, but some speculations are possible. This outer pore residue may regulate the flexibility of the selectivity filter directly, perhaps by affecting the interaction between the residues of selectivity filter and the pore helix (Cordero-Morales et al., 2007). Alternatively, the action of Y407/444 in Kv3 channels may be indirect, as in Kv1.5 where the mutation of R487 to Y or V reduces C-type inactivation of the selectivity filter. In this case, the presence of Y407/444 may prevent Kv3.1/3.2b channels from undergoing the conformational changes associated with C-type inactivation, and this might reduce the ability of the pore to cut off the permeation of larger ions. In native Kv3 channels, the selectivity filter may remain in a more flexible

open state, allowing $NMDG^+$ ions to enter and then expand the pore to go through.

The authors thank Dr. D. Steele for expert technical assistance in preparing channel constructs and Fifi Chiu and Kyung Hee Park for help with cell culture.

This work was supported by operating grants to D. Fedida and S.J. Kehl from the Canadian Institutes of Health Research and the Heart and Stroke Foundation of B.C. & Yukon.

Edward N. Pugh Jr. served as editor.

Submitted: 9 October 2008
Accepted: 5 March 2009

REFERENCES

Bezanilla, F., and C.M. Armstrong. 1972. Negative conductance caused by entry of sodium and cesium ions into the potassium channels of squid axons. *J. Gen. Physiol.* 60:588–608.

Bezanilla, F., E. Perozo, and E. Stefani. 1994. Gating of *Shaker* K^+ channels: II. The components of gating currents and a model of channel activation. *Biophys. J.* 66:1011–1021.

Brew, H.M., and I.D. Forsythe. 1995. Two voltage-dependent K^+ conductances with complementary functions in postsynaptic integration at a central auditory synapse. *J. Neurosci.* 15:8011–8022.

Castle, N.A., S.R. Fadous, D.E. Logothetis, and G.K. Wang. 1994. 4-aminopyridine binding and slow inactivation are mutually exclusive in rat Kv1.1 and *Shaker* potassium channels. *Mol. Pharmacol.* 46:1175–1181.

Chen, F.S., D. Steele, and D. Fedida. 1997. Allosteric effects of permeating cations on gating currents during K^+ channel deactivation. *J. Gen. Physiol.* 110:87–100.

Ciani, S., K. Nishikawa, and Y. Kidokoro. 1997. Permeation of organic cations and ammonium through the glutamate receptor channel in *Drosophila* larval muscle. *Jpn. J. Physiol.* 47:189–198.

Cordero-Morales, J.F., V. Jogini, A. Lewis, V. Vasquez, D.M. Cortes, B. Roux, and E. Perozo. 2007. Molecular driving forces determining potassium channel slow inactivation. *Nat. Struct. Mol. Biol.* 14:1062–1069.

Doyle, D.A., J.M. Cabral, R.A. Pfuetzner, A.L. Kuo, J.M. Gulbis, S.L. Cohen, B.T. Chait, and R. MacKinnon. 1998. The structure of the potassium channel: molecular basis of K^+ conduction and selectivity. *Science.* 280:69–77.

Eickhorst, A.N., A. Berson, D. Cockayne, H.A. Lester, and B.S. Khakh. 2002. Control of $P2X_2$ channel permeability by the cytosolic domain. *J. Gen. Physiol.* 120:119–131.

Fedida, D., B. Wible, Z. Wang, B. Fermini, F. Faust, S. Nattel, and A.M. Brown. 1993. Identity of a novel delayed rectifier current from human heart with a cloned K^+ channel current. *Circ. Res.* 73:210–216.

Fedida, D., R. Bouchard, and F.S.P. Chen. 1996. Slow gating charge immobilization in the human potassium channel Kv1.5 and its prevention by 4-aminopyridine. *J. Physiol.* 494:377–387.

Fedida, D., N.D. Maruoka, and S. Lin. 1999. Modulation of slow inactivation in human cardiac Kv1.5 channels by extra- and intracellular permeant cations. *J. Physiol.* 515:315–329.

Friederich, P., J.P. Dilger, D. Isbrandt, K. Sauter, O. Pongs, and B.W. Urban. 2003. Biophysical properties of Kv3.1 channels in SH-SY5Y human neuroblastoma cells. *Receptors Channels.* 9:387–396.

Fujiwara, Y., and Y. Kubo. 2006. Regulation of the desensitization and ion selectivity of ATP-gated P2X2 channels by phosphoinositides. *J. Physiol.* 576:135–149.

Hackos, D.H., T.H. Chang, and K.J. Swartz. 2002. Scanning the intracellular S6 activation gate in the *Shaker* K^+ channel. *J. Gen. Physiol.* 119:521–532.

Harris, R.E., and E.Y. Isacoff. 1996. Hydrophobic mutations alter the movement of Mg^{2+} in the pore of voltage-gated potassium channels. *Biophys. J.* 71:209–219.

Heinemann, S.H., F. Conti, and W. Stuhmer. 1992. Recording of gating currents from *Xenopus* oocytes and gating noise analysis. *Methods Enzymol.* 207:353–368.

Hille, B. 1973. Potassium channels in myelinated nerve. Selective permeability to small cations. *J. Gen. Physiol.* 61:669–686.

Hille, B. 2001. Ionic Channels of Excitable Membranes. 3rd ed. Sinauer Associates Inc., Sunderland, MA. 814 pp.

Horie, M., H. Irisawa, and A. Noma. 1987. Voltage-dependent magnesium block of adenosine-triphosphate-sensitive potassium channel in guinea-pig ventricular cells. *J. Physiol.* 387:251–272.

Jordan, P.C. 2007. Tuning a potassium channel–the caress of the surroundings. *Biophys. J.* 93:1091–1092.

Kavanaugh, M.P., M.D. Varnum, P.B. Osborne, M.J. Christie, A.E. Busch, J.P. Adelman, and R.A. North. 1991. Interaction between tetraethylammonium and amino acid residues in the pore of cloned voltage-dependent potassium channels. *J. Biol. Chem.* 266:7583–7587.

Khakh, B.S., X.R. Bao, C. Labarca, and H.A. Lester. 1999. Neuronal P2X transmitter-gated cation channels change their ion selectivity in seconds. *Nat. Neurosci.* 2:322–330.

Khodakhah, K., A. Melishchuk, and C.M. Armstrong. 1997. Killing K channels with TEA^+. *Proc. Natl. Acad. Sci. USA.* 94:13335–13338.

Kiss, L., J. LoTurco, and S.J. Korn. 1999. Contribution of the selectivity filter to inactivation in potassium channels. *Biophys. J.* 76:253–263.

Lawonn, P., E.K. Hoffmann, C. Hougaard, and F. Wehner. 2003. A cell shrinkage-induced non-selective cation conductance with a novel pharmacology in Ehrlich-Lettre-ascites tumour cells. *FEBS Lett.* 539:115–119.

Lenaeus, M.J., M. Vamvouka, P.J. Focia, and A. Gross. 2005. Structural basis of TEA blockade in a model potassium channel. *Nat. Struct. Mol. Biol.* 12:454–459.

Li, Q., X. Luo, and S. Muallem. 2005. Regulation of the P2X7 receptor permeability to large molecules by extracellular Cl^- and Na^+. *J. Biol. Chem.* 280:26922–26927.

Li, T., F. ter Veld, H.R. Nurnberger, and F. Wehner. 2005. A novel hypertonicity-induced cation channel in primary cultures of human hepatocytes. *FEBS Lett.* 579:2087–2091.

Lien, C.C., and P. Jonas. 2003. Kv3 potassium conductance is necessary and kinetically optimized for high-frequency action potential generation in hippocampal interneurons. *J. Neurosci.* 23:2058–2068.

Lippiat, J.D., N.B. Standen, and N.W. Davies. 1998. Block of cloned BK_{Ca} channels (*rSlo*) expressed in HEK 293 cells by N-methyl D-glucamine. *Pflugers Arch.* 436:810–812.

Liu, Y., M.E. Jurman, and G. Yellen. 1996. Dynamic rearrangement of the outer mouth of a K^+ channel during gating. *Neuron.* 16:859–867.

Loboda, A., and C.M. Armstrong. 2001. Resolving the gating charge movement associated with late transitions in K channel activation. *Biophys. J.* 81:905–916.

Long, S.B., E.B. Campbell, and R. MacKinnon. 2005. Crystal structure of a mammalian voltage-dependent *Shaker* family K^+ channel. *Science.* 309:897–903.

Lopez-Barneo, J., T. Hoshi, S.H. Heinemann, and R.W. Aldrich. 1993. Effects of external cations and mutations in the pore region on C-type inactivation of *Shaker* potassium channels. *Receptors Channels.* 1:61–71.

Luneau, C., R. Wiedmann, J.S. Smith, and J.B. Williams. 1991a. Shaw-like rat brain potassium channel cDNA's with divergent 3′ ends. *FEBS Lett.* 288:163–167.

Luneau, C.J., J.B. Williams, J. Marshall, E.S. Levitan, C. Oliva, J.S. Smith, J. Antanavage, K. Folander, R.B. Stein, and R. Swanson. 1991b. Alternative splicing contributes to K^+ channel diversity in

the mammalian central nervous system. *Proc. Natl. Acad. Sci. USA.* 88:3932–3936.

Lunin, V.V., E. Dobrovetsky, G. Khutoreskaya, R. Zhang, A. Joachimiak, D.A. Doyle, A. Bochkarev, M.E. Maguire, A.M. Edwards, and C.M. Koth. 2006. Crystal structure of the CorA Mg^{2+} transporter. *Nature.* 440:833–837.

Ma, W., A. Korngreen, S. Weil, E.B. Cohen, A. Priel, L. Kuzin, and S.D. Silberberg. 2006. Pore properties and pharmacological features of the P2X receptor channel in airway ciliated cells. *J. Physiol.* 571:503–517.

MacKinnon, R., and G. Yellen. 1990. Mutations affecting TEA blockade and ion permeation in voltage-activated K^+ channels. *Science.* 250:276–279.

Matsuda, H., A. Saigusa, and H. Irisawa. 1987. Ohmic conductance through the inwardly rectifying K channel and blocking by internal Mg^{2+}. *Nature.* 325:156–159.

McCormack, K., W.J. Joiner, and S.H. Heinemann. 1994. A characterization of the activating structural rearrangements in voltage-dependent *Shaker* K^+ channels. *Neuron.* 12:301–315.

Melishchuk, A., and C.M. Armstrong. 2001. Mechanism underlying slow kinetics of the OFF gating current in *Shaker* potassium channel. *Biophys. J.* 80:2167–2175.

Nichols, C.G., and A.N. Lopatin. 1997. Inward rectifier potassium channels. *Annu. Rev. Physiol.* 59:171–191.

Nilius, B., R. Vennekens, J. Prenen, J.G. Hoenderop, R.J. Bindels, and G. Droogmans. 2000. Whole-cell and single channel monovalent cation currents through the novel rabbit epithelial Ca^{2+} channel ECaC. *J. Physiol.* 527:239–248.

Noda, M., S. Shimizu, T. Tanabe, T. Takai, T. Kayano, T. Ideda, H. Takahashi, H. Nakayama, Y. Kanaoka, N. Minamino, et al. 1984. Primary structure of *Electrophorus electricus* sodium channel deduced from cDNA sequence. *Nature.* 312:121–127.

Papazian, D.M., L.C. Timpe, Y.N. Jan, and L.Y. Jan. 1991. Alteration of voltage-dependence of *Shaker* potassium channel by mutations in the S4 sequence. *Nature.* 349:305–310.

Perney, T.M., and L.K. Kaczmarek. 1997. Localization of a high threshold potassium channel in the rat cochlear nucleus. *J. Comp. Neurol.* 386:178–202.

Perozo, E., D.M. Papazian, E. Stefani, and F. Bezanilla. 1992. Gating currents in *Shaker* K^+ channels. Implications for activation and inactivation models. *Biophys. J.* 62:160–168.

Perozo, E., R. MacKinnon, F. Bezanilla, and E. Stefani. 1993. Gating currents from a non-conducting mutant reveal open-closed conformation in *Shaker* K^+ channels. *Neuron.* 11:353–358.

Perozo, E., L. Santacruz-Toloza, E. Stefani, F. Bezanilla, and D.M. Papazian. 1994. S4 mutations alter gating currents of *Shaker* K channels. *Biophys. J.* 66:345–354.

Rudy, B., and C.J. McBain. 2001. Kv3 channels: voltage-gated K^+ channels designed for high-frequency repetitive firing. *Trends Neurosci.* 24:517–526.

Rudy, B., A. Chow, D. Lau, Y. Amarillo, A. Ozaita, M. Saganich, H. Moreno, M.S. Nadal, R. Hernandez-Pineda, A. Hernandez-Cruz, et al. 1999. Contributions of Kv3 channels to neuronal excitability. *Ann. NY Acad. Sci.* 868:304–343.

Shao, X.M., and D.M. Papazian. 1993. S4 mutations alter the single-channel gating kinetics of *Shaker* K^+ channels. *Neuron.* 11:343–352.

Shealy, R.T., A.D. Murphy, R. Ramarathnam, E. Jakobsson, and S. Subramaniam. 2003. Sequence-function analysis of the K^+-selective family of ion channels using a comprehensive alignment and the KcsA channel structure. *Biophys. J.* 84:2929–2942.

Shiga, N., and P. Wangemann. 1995. Ion selectivity of volume regulatory mechanisms present during a hypoosmotic challenge in vestibular dark cells. *Biochim. Biophys. Acta.* 1240:48–54.

Sokolov, S., T. Scheuer, and W.A. Catterall. 2007. Gating pore current in an inherited ion channelopathy. *Nature.* 446:76–78.

Southan, A.P., and B. Robertson. 2000. Electrophysiological characterization of voltage-gated K^+ currents in cerebellar basket and Purkinje cells: Kv1 and Kv3 channel subfamilies are present in basket cell nerve terminals. *J. Neurosci.* 20:114–122.

Starkus, J.G., L. Kuschel, M.D. Rayner, and S.H. Heinemann. 1997. Ion conduction through C-type inactivated *Shaker* channels. *J. Gen. Physiol.* 110:539–550.

Starkus, J.G., L. Kuschel, M.D. Rayner, and S.H. Heinemann. 1998. Macroscopic Na^+ currents in the "nonconducting" *Shaker* potassium channel mutant W434F. *J. Gen. Physiol.* 112:85–93.

Varma, S., and S.B. Rempe. 2007. Tuning ion coordination architectures to enable selective partitioning. *Biophys. J.* 93:1093–1099.

Villarroel, A., N. Burnashev, and B. Sakmann. 1995. Dimensions of the narrow portion of a recombinant NMDA receptor channel. *Biophys. J.* 68:866–875.

Virginio, C., A. MacKenzie, F.A. Rassendren, R.A. North, and A. Surprenant. 1999. Pore dilation of neuronal P2X receptor channels. *Nat. Neurosci.* 2:315–321.

Wang, Z., and D. Fedida. 2001. Gating charge immobilization caused by the transition between inactivated states in the Kv1.5 channel. *Biophys. J.* 81:2614–2627.

Wang, Z., and D. Fedida. 2002. Uncoupling of gating charge movement and closure of the ion pore during recovery from inactivation in the Kv1.5 channel. *J. Gen. Physiol.* 120:249–260.

Wang, Z., X. Zhang, and D. Fedida. 1999. Gating current studies reveal both intra- and extra-cellular cation modulation of K^+ channel deactivation. *J. Physiol.* 515:331–339.

Wang, Z., J.C. Hesketh, and D. Fedida. 2000a. A high-Na^+ conduction state during recovery from inactivation in the K^+ channel Kv1.5. *Biophys. J.* 79:2416–2433.

Wang, Z., X. Zhang, and D. Fedida. 2000b. Regulation of transient Na^+ conductance by intra- and extracellular K^+ in the human delayed rectifier K^+ channel Kv1.5. *J. Physiol.* 523:575–591.

Yang, X.-C., and F. Sachs. 1990. Characterization of stretch-activated ion channels in *Xenopus* oocytes. *J. Physiol.* 431:103–122.

Yang, Y., Y. Yan, and F.J. Sigworth. 1997. How does the W434F mutation block current in *Shaker* potassium channels? *J. Gen. Physiol.* 109:779–789.

Zhang, Z., and C.W. Bourque. 2006. Calcium permeability and flux through osmosensory transduction channels of isolated rat supraoptic nucleus neurons. *Eur. J. Neurosci.* 23:1491–1500.

Zheng, J., and F.J. Sigworth. 1997. Selectivity changes during activation of mutant *Shaker* potassium channels. *J. Gen. Physiol.* 110:101–117.

Zheng, J., and F.J. Sigworth. 1998. Intermediate conductances during deactivation of heteromultimeric *Shaker* potassium channels. *J. Gen. Physiol.* 112:457–474.